Development of an achromatic full-field hard X-ray microscope using two monolithic imaging mirrors

S. Matsuyama*[a], H. Kino[a], S. Yasuda[a], Y. Kohmura[b], H. Okada[c],
M. Yabashi[b], T. Ishikawa[b], K. Yamauchi[a]
[a]Department of Precision Science and Technology, Graduate School of Engineering,
Osaka University, 2-1 Yamadaoka, Suita, Osaka 565-0871, Japan
[b]RIKEN SPring-8 Center, 1-1-1, Kouto, Sayo-cho, Sayo-gun, Hyogo 679-5148, Japan
[c]JTEC Corporation, 2-4-35, Yamabuki Saito, Ibaraki, Osaka 567-0086, Japan

ABSTRACT

Advanced Kirkpatrick-Baez mirror optics using two monolithic imaging mirrors was developed to realize an achromatic, high-resolution, and a high-stability full-field X-ray microscope. The mirror consists of an elliptical section and a hyperbolic section on a quartz glass substrate, in which the geometry follows the Wolter (type I) optics rules. A preliminary test was performed at SPring-8 using X-rays monochromatized to 9.881 keV. A 100-nm feature on a Siemens star chart could be clearly observed.

Keywords: X-ray microscopy, X-ray mirror, achromatic imaging, advanced Kirkpatrick-Baez mirror optics

1. INTRODUCTION

X-ray microscopy has great potential to allow the observation of a sample at better resolution than several tens of nanometers and to allow analysis of a sample while visualizing the nanostructure. Additionally, because of the high penetration power of hard X-rays, the inside of relatively thick samples and samples in aqueous and/or gaseous environments can be observed, samples which cannot be resolved by electron microscopes. For example, these advantages allow one to observe the inside of operating batteries and catalysts at high resolution.

For the development of a full-field hard X-ray microscope, a Fresnel zone plate (FZP) is typically used because very fine FZPs can be fabricated[1-3]. Because of the high performance of FZPs, a very high-resolution X-ray microscope can be developed without any technological difficulties. According to several studies conducted on Fresnel zone plates[2,3], the state-of-the-art FZP can reach a 20-nm resolution, even in the hard X-ray region of 8 keV. However, a FZP is not ideal for spectromicroscopy because it has strong chromatic aberration, which changes the focal length based on the wavelength of incident X-rays. Thus, achromatic imaging optics is desired for such applications.

We have developed an achromatic optical imaging system based on four total-reflection mirrors, i.e., using advanced Kirkpatrick-Baez (KB) mirror optics[4-7]. In our previous work[7], roughly 100-nm spatial resolution without chromatic aberration was achieved. Recently, we improved advanced KB mirror optics to develop a higher-resolution, easy-to-use, high-stability microscope. To meet such specifications, a monolithic mirror combined with an elliptical mirror and a hyperbolic mirror, which can function as one-dimensional imaging optics, is one of the solutions. This monolithic structure makes the imaging system very stable and easy-to-use because the relative alignment between the ellipse and the hyperbola is fixed, although it is very sensitive to the point spread function of the imaging system. From the viewpoint of engineering, mirror fabrication is relatively easy, unlike for a Wolter mirror[8], which consists of an ellipsoid and a hyperboloid.

In this paper, we report results of preliminary imaging tests using the developed monolithic imaging mirrors. A full-field microscope was constructed at SPring-8 for the test. A Siemens star chart with a minimum feature size of 100 nm was observed at an X-ray energy of 9.881 keV.

*matsuyama@prec.eng.osaka-u.ac.jp; phone +81-6-6879-7286, http://www.dma.jim.osaka-u.ac.jp/view?l=en&u=4001

X-Ray Nanoimaging: Instruments and Methods II, edited by Barry Lai,
Proc. of SPIE Vol. 9592, 959208 · © 2015 SPIE · CCC code:
0277-786X/15/$18 · doi: 10.1117/12.2188583

2. EXPERIMENTAL SETUP FOR IMAGING TEST

The monolithic one-dimensional imaging mirror consists of an elliptical shape and a hyperbolic shape on a single substrate, for which the geometry followed the Wolter (type I) optics rule (Fig. 1). Detailed parameters are provided in Table 1. The imaging optical system has a working distance of 34 mm and a numerical aperture of 1.44 and 1.51 mrad in the vertical and horizontal directions, respectively. The magnification factors are 196 and 637 in the vertical and horizontal directions, respectively. The mismatched magnifications caused by the different focal lengths of the vertical and horizontal imaging systems are digitally corrected after taking an image.

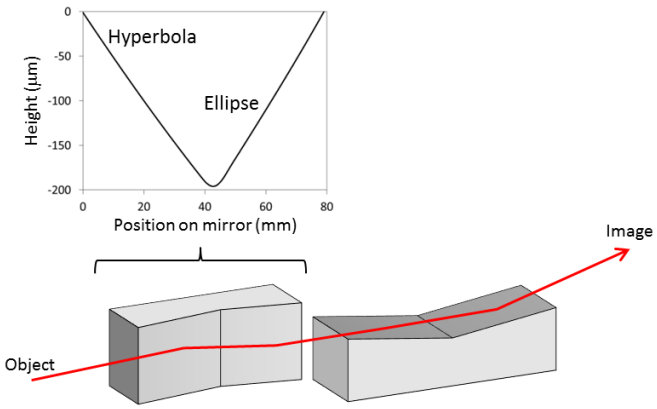

Figure 1. Advanced Kirkpatrick-Baez mirror optics using two monolithic one-dimensional imaging mirrors

Table 1. Parameters of the developed advanced Kirkpatrick-Baez mirror optics

	Vertical imaging		Horizontal imaging	
Shape	Hyperbola	Ellipse	Hyperbola	Ellipse
Incident glancing angle (mrad)*	4.7	5.5	4.6	5.5
Area length (mm)	100	120	30	39
Magnification factor	196		637	
Numerical aperture ($\times 10^{-3}$)	1.44		1.51	

*At the center of the mirror.

The substrate material is quartz glass with dimensions of 232 × 50 × 30 mm^3 and 80 × 50 × 30 mm^3 for the vertical and horizontal imaging mirrors, respectively. Each mirror shape (the elliptical part and the hyperbolic part) was measured with our two home-made stitching interferometers with an accuracy of roughly 1 nm[9,10]. However, the entire shape, which bears resemblance to a "V", was measured using a coordinate-measuring machine, because the steeply curved "V" shape cannot be measured using an interferometer. The shape data obtained using the stitching interferometers and the coordinate measuring machine was combined into a single shape data set. Based on the shape data, the mirrors were finely fabricated using computer-controlled elastic emission machining (EEM)[11]. The mirrors could be fabricated with a shape accuracy of 2 nm or better (from peak-to-valley). The details of the fabrication are under preparation for publication. The accuracy was sufficiently good to form an image without blurring (caused by imperfections introduced during the mirror fabrication), according to results calculated by our developed wave-optical simulator[12]. The surface roughness of the processed area is approximately 0.2 nm rms, which is sufficient to retain ideal reflectivity. After the shape correction, the effective reflection area was covered with a roughly 100-nm-thick layer of platinum using a magnetron sputtering deposition system. There is no difference between the shapes before and after the deposition.

The first imaging test was performed at BL29XUL of SPring-8. The X-ray energy was monochromatized to 9.881 keV using a double crystal monochromator [Si(111)]. The experimental setup consists of a rotating diffuser, a polycapillary lens, the developed imaging mirrors, a 45-m-long vacuum duct, and an X-ray camera (see Fig. 2). The rotating diffuser (paper) is installed to suppress unwanted interference. The polycapillary lens with a focal length of 45 mm, which is defined as the distance between the end of the lens and the focal point was employed; its external dimension is 41 mm (length) × 4 mm (diameter). Therefore, the maximum numerical aperture is roughly 31×10^{-3}, if the entire entrance is illuminated. The lens is used for the following purposes (i.e., apart from being used as a condenser to increase the signals at the camera). One use is for incoherent illumination. General bright-field imaging needs incoherent illumination to improve spatial resolution. If the degree of coherence is small, unwanted interference among different points occurs, which results in degradation of spatial resolution. To create incoherent illumination, the numerical aperture of the lens was set to the same value as that of the imaging mirror with a cross slit. The other use is as a deflector. In grazing-incidence reflective optics, the trajectory of rays after reflection is slightly inclined; the inclined angle is double the grazing incidence angle. In our case, the total grazing-incidence angle of the imaging mirror is approximately 10 mrad in both directions. Therefore, passing the rays after reflection by the imaging mirrors through the long vacuum duct is impossible, unless the beam is inclined so as to cancel the 20-mrad deflection. The outermost region of the polycapillary lens was used to incline the incident beam by 20 mrad (see Fig. 3). The two imaging mirrors were arranged perpendicularly to construct the advanced Kirkpatrick-Baez geometry. The perpendicularity was adjusted using a pentaprism and two autocollimators, following the alignment procedure for KB mirrors[13]. The X-ray camera was placed at the third experimental hutch, which is roughly 98 m from the light-source undulator and roughly 45 m from the imaging mirror. The device consists of a thin scintillator (P43) with a thickness of 10 μm, a lens (×2.1), and a CMOS sensor (2048 × 2048 pixels, 6.5 μm/pixel). The effective pixel size through the lens is 3.1 μm.

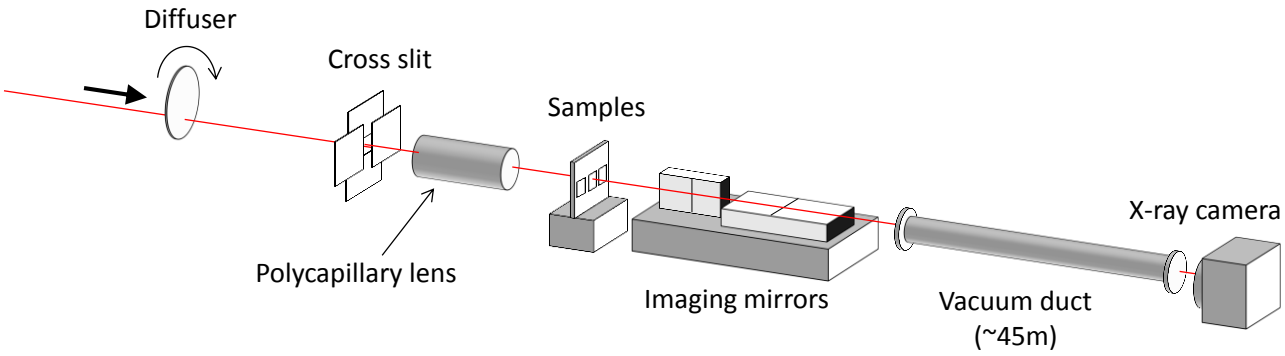

Figure 2. Experimental setup of the full-field X-ray microscope.

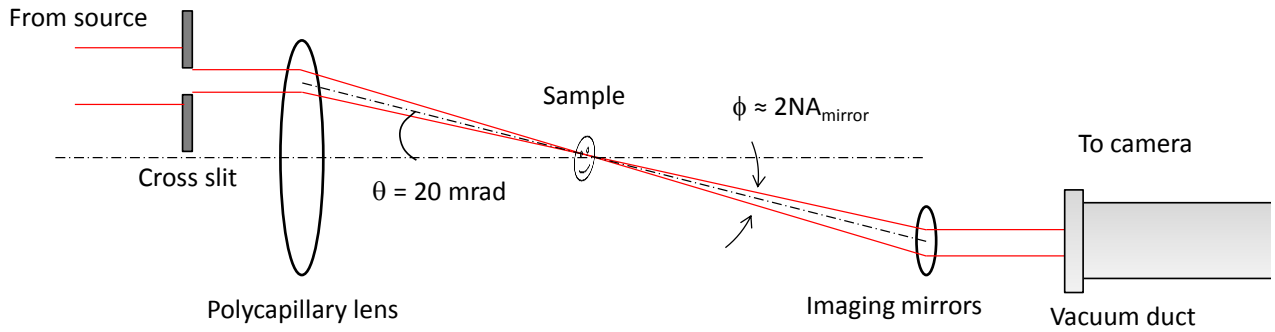

Figure 3. Ray diagram around a sample.

The incident angle of the imaging mirrors was adjusted to match the center of field of view of the imaging system to the center of the camera. The focal length was simultaneously adjusted. An important point of these adjustments is to utilize the field curvature of the imaging mirror. The imaging mirror has field curvature, which was reported in our previous paper[4]. We can find both the best focus and the center of the field by adjusting both the focal length and the incident angle of the imaging mirrors while checking the position of the best focus region on the camera.

3. RESULTS AND DISCUSSION

First, the polycapillary lens was characterized using 10-keV X-rays. The adjustment was quickly completed because only the incident angle was adjusted. At the center region of the lens, the X-ray could be focused down to roughly 60 μm. The throughput was roughly 80%. However, in the outermost region, which can incline the beam by 20 mrad, the achieved focus size was roughly 120 μm and the throughput was roughly 15%, which might not be sufficiently reliable because these properties significantly depend on the condition of the adjustment. This result suggests that, for practical purposes, the lens must be improved in terms of focus size and throughput at the outermost region. However, as a test to characterize an imaging mirror, this system is very convenient in terms of ease of alignment and stability.

As a preliminary test, a Siemens star chart (which is made of tantalum, and has a thickness of 1 μm and a minimum line width of 100 nm), was observed. Figure 4 shows the bright field image of the chart. The exposure time is 10 s. The image was processed using both the flat field correction to remove the effect of non-uniform illumination and the magnification correction to remove the mismatched magnification of the vertical and horizontal directions. As can be seen in the center region, 100-nm features can be clearly resolved. Additionally, there is no distortion, even at the outside region. The dark and white contrast is highly binarized, which suggests that the sample was illuminated incoherently (as expected).

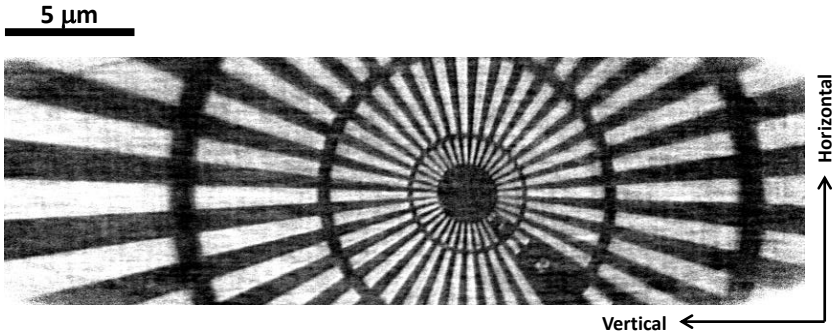

Figure 4. Bright field X-ray image of a Siemens star chart. X-ray energy = 9.881 keV. Exposure time = 10 s. The innermost region has 100-nm features.

4. SUMMARY AND OUTLOOK

We developed an achromatic, high-resolution full-field X-ray microscope with two monolithic one-dimensional imaging mirrors. The imaging mirrors were successfully fabricated with a shape that is accurate upto 2 nm. In the first test, the 100-nm features of the test chart could be clearly visualized. In future tests, we will investigate the minimum spatial resolution using a fine Siemens star chart with 50-nm features. Thereafter, we will apply this microscope to spectromicroscopy in the X-ray region, such as in XAFS imaging and full-field X-ray fluorescence imaging.

ACKNOWLEDGEMENTS

This research was supported by the SENTAN project of JST. It was partially supported by JSPS KAKENHI (Grant Nos. 26286077, 23226004), the CREST project of JST, and Konica Minolta Imaging Science Foundation. The use of BL29XUL at SPring-8 was supported by RIKEN. We acknowledge K. Tamasaku for his valuable discussions.

REFERENCES

[1] Suzuki, Y., Takeuchi, A., Takenaka, H., and Okada, I., "Fabrication and performance test of Fresnel zone plate with 35 nm outermost zone width in hard X-ray region," X-Ray Opt. Instrum. 2010, 1–6 (2010).

[2] Chen, T.-Y., Chen, Y.-T., Wang, C.-L., Kempson, I.M., Lee, W.-K., Chu, Y.S., Hwu, Y., and Margaritondo, G., "Full-field microimaging with 8 keV X-rays achieves a spatial resolutions better than 20 nm.," Opt. Express 19(21), 19919–24 (2011).

[3] Vila-Comamala, J., Pan, Y., Lombardo, J.J., Harris, W.M., Chiu, W.K.S., David, C., and Wang, Y., "Zone-doubled Fresnel zone plates for high-resolution hard X-ray full-field transmission microscopy.," J. Synchrotron Radiat. 19(5), 705–9 (2012).

[4] Matsuyama, S., Wakioka, T., Kidani, N., Kimura, T., Mimura, H., Sano, Y., Nishino, Y., Yabashi, M., Tamasaku, K., et al., "One-dimensional Wolter optics with a sub-50 nm spatial resolution.," Opt. Lett. 35(21), 3583–5 (2010).

[5] Matsuyama, S., Kidani, N., Mimura, H., Sano, Y., Kohmura, Y., Tamasaku, K., Yabashi, M., Ishikawa, T., and Yamauchi, K., "Hard-X-ray imaging optics based on four aspherical mirrors with 50 nm resolution," Opt. Express 20(9), 10310–9 (2012).

[6] Matsuyama, S., Emi, Y., Kino, H., Kohmura, Y., Yabashi, M., Ishikawa, T., and Yamauchi, K., "Development of achromatic full-field hard x-ray microscopy and its application to x-ray absorption near edge structure spectromicroscopy," Proc. SPIE 9207, 92070Q (2014).

[7] Matsuyama, S., Emi, Y., Kino, H., Kohmura, Y., Ishikawa, T., and Yamauchi, K., "Achromatic and high-resolution full-field X-ray microscopy based on total-reflection mirrors," Opt. Express 23(8), 9746–9752 (2015).

[8] Wolter, H., "Spiegelsysteme streifenden Einfalls als abbildende Optiken für Röntgenstrahlen," Ann. Phys. 445(1-2), 94–114 (1952).

[9] Yamauchi, K., Yamamura, K., Mimura, H., Sano, Y., Saito, A., Ueno, K., Endo, K., Souvorov, A., Yabashi, M., Tamasaku, K., Ishikawa, T., Mori, Y. Tamasaku, K., Nishino, Y., Ishikawa, T., and Yamauchi, K., "Microstitching interferometry for x-ray reflective optics," Rev. Sci. Instrum. 74(5), 2894 (2003).

[10] Mimura, H., Yumoto, H., Matsuyama, S., Yamamura, K., Sano, Y., Ueno, K., Endo, K., Mori, Y., Yabashi, M., et al., "Relative angle determinable stitching interferometry for hard x-ray reflective optics," Rev. Sci. Instrum. 76(4), 045102 (2005).

[11] Yamauchi, K., Mimura, H., Inagaki, K., and Mori, Y., "Figuring with subnanometer-level accuracy by numerically controlled elastic emission machining," Rev. Sci. Instrum. 73(11), 4028 (2002).

[12] Matsuyama, S., Fujii, M., and Yamauchi, K., "Simulation study of four-mirror alignment of advanced Kirkpatrick−Baez optics," Nucl. Instrum. Methods Phys. Res. Sect. A 616(2-3), 241–245 (2010).

[13] Matsuyama, S., Mimura, H., Yumoto, H., Hara, H., Yamamura, K., Sano, Y., Endo, K., Mori, Y., Yabashi, M., Nishino, Y., Tamasaku, K., Ishikawa, T., Yamauchi, K., "Development of mirror manipulator for hard-x-ray nanofocusing at sub-50-nm level," Rev. Sci. Instrum. 77(9), 093107 (2006).